Segmental Flexibility of Immunoglobulin G Antibody Molecules in Solution: A New Interpretation†

Douglas C. Hanson, Juan Yguerabide, and Verne N. Schumaker*

ABSTRACT: We propose a new model for the segmental flexibility of immunoglobulin G (IgG). The flexibility of native and mildly reduced anti-5-(dimethylamino)naphthalene-1-sulfonyl (anti-dansyl) antibody was reexamined by nanosecond fluorescence spectroscopy using deconvolution and lamp-shift corrections. The rabbit antibodies used for this study were purified of dimers and other aggregates. The original results indicated that the decay of fluorescence anisotropy involved two rotational correlation times. It was suggested that the short rotational correlation time, ϕ_s, represented a flexible Fab arm motion over a restricted angle and that the long correlation time, ϕ_L, represented global tumbling of the molecule [Yguerabide, J., Epstein, H. F., & Stryer, L. (1970) *J. Mol. Biol. 51*, 573–590]. Our new data indicate that the long correlation time primarily represents motions of the Fab segments and *not* global tumbling of the entire molecule. This interpretation implies a more flexible model for IgG. Thus, in solution the antibody arms appear to move over a wide angle and are not restricted to 33° as was suggested in the earlier model. Simple diffusion calculations and other evidence suggest that ϕ_s may represent V-module flexibility about the switch peptides or Fab twisting around its long axis, whereas ϕ_L may represent wagging or wobbling motions of the Fab arms about the hinge region. The faster motions appear to occur over small angles whereas the slower wagging or wobbling motions responsible for most of the decay of anisotropy appear to be much less restricted. The biological function of IgG and anisotropy changes resulting from hinge disulfide cleavage are interpreted in terms of the proposed model. We also demonstrate a useful method for comparison of time-dependent and steady-state fluorescence polarization data.

The ability of immunoglobulin G (IgG)[1] antibody molecules to form complexes with antigens of vastly different topographies has been attributed to their segmental flexibility (Noelken et al., 1965; Feinstein & Rowe, 1965). Because of the wide variety of biological functions triggered by these antibody–antigen complexes (Metzger, 1974, 1978), it is important to understand the dynamic properties that apparently facilitate their formation. With amazing insight, Noelken et al. (1965) proposed a model for IgG consisting of three compact globular regions joined by two flexible polypeptide chains held together by a disulfide bond. Two years later, Valentine & Green (1967) published their classic electron microscopy study of ring-shaped polymers of IgG held together by small bivalent haptens. From this study, it was inferred that the hapten binding sites were located at the ends of the Fab arms and that the Fab segments were joined by a hinge that allowed the arms to assume angles from nearly 0 to 180°. Figure 1 illustrates several possible modes of Fab arm flexibility.

A variety of conflicting steady-state polarization studies failed to clearly detect the antibody's flexibility in solution (Metzger, 1974; Dandliker & de Saussure, 1970). The studies were frustrated by the independent rotation of covalently attached fluorescent probes and by the inability of the technique to resolve different depolarizing motions. Advances in the generation and detection of nanosecond light pulses soon made it possible to directly measure the time dependence of fluorescence intensity following a fast pulse of light.

In 1970, Yguerabide et al. used nanosecond fluorescence spectroscopy to detect the segmental flexibility of antibody molecules in solution. Problems associated with probe wiggle were eliminated by using antibody directed against a dansyl fluorophore. Analysis of raw anisotropy curves clearly demonstrated the presence of at least two separate depolarizing motions. The shorter rotational correlation time of 33 ns was attributed to flexible motions of the Fab segments over a restricted angle; the longer correlation time of 168 ns was attributed to global tumbling of the entire molecule. Brochon et al. (1972) used time-dependent spectroscopy to study covalent dansyl-IgG conjugates. These workers found a long correlation time of about 100 ns and also concluded that ϕ_L "is due to a global motion of the molecules". Probe wiggle was most likely responsible for the low ϕ_s of only a few nanoseconds observed for these covalent conjugates. More recently, Chan & Cathou (1977) performed nanosecond measurements on anti-dansyl antibody carefully purified of aggregates and found a ϕ_L of only 109 ns. They interpreted their results in terms of the model first suggested by Yguerabide et al. (1970). Lovejoy et al. (1977) performed time-dependent measurements on anti-pyrene antibodies. Use of the long-lifetime pyrene probe extended the range of anisotropy decay from about 120 ns to nearly 350 ns. The extended curve showed no tendency to rise with longer time, and the decay profile was similar to the anti-dansyl antibody decay reported by Chan & Cathou (1977). The authors concluded that the longer rotational correlation time "probably represents global motion of the entire molecule". Of interest, the segmental flexibility was increased after selective reduction of IgG's inter-heavy-chain disulfide bond (Romans et al., 1977; Chan & Cathou, 1977; Seegan et al., 1979).

† From the Department of Chemistry and the Molecular Biology Institute, University of California, Los Angeles, California 90024 (D.C.H. and V.N.S.), and the Department of Biology, University of California, San Diego, La Jolla, California 92093 (J.Y.). *Received May 14, 1981.* Supported in part by National Science Foundation Grant PCM 77-17577. An abbreviated account of this work was presented at the Joint Meeting of the Swiss Society for Biochemistry and the German Society for Biological Chemistry, Basel, July 1980 (Hanson et al., 1981a), and at the 72nd Annual Meeting of the American Society of Biological Chemists, St. Louis, MO, June 1981 (Hanson et al., 1981b).

[1] Abbreviations used: IgG, immunoglobulin G; dansyl, 5-(dimethylamino)naphthalene-1-sulfonyl; PBS, 0.01 M potassium phosphate–0.15 M NaCl buffer, pH 7.4; SAS, saturated ammonium sulfate; $NaDodSO_4$, sodium dodecyl sulfate.

0006-2960/81/0420-6842$01.25/0

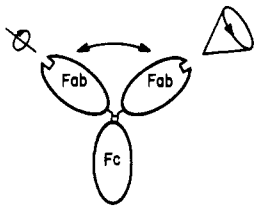

FIGURE 1: Some likely twisting, wagging, and conelike wobbling motions of the Fab arms of IgG. (Possible V-module flexibility is not shown.)

In this study, we used nanosecond spectroscopy to carefully reexamine the segmental flexibility of native and mildly reduced and alkylated anti-dansyl antibody. Data analysis was performed by the method of moments with deconvolution and lamp-shift corrections. On the basis of these new data and theoretical calculations, we contend that both the short and the long rotational correlation times are principally due to flexible motions of the antibody arms. This interpretation implies a more flexible model for IgG in which the antibody arms are free to move over a wide angle.

Experimental Procedures

Anti-Dansyl Antibody. The protein conjugates dansyl$_{10}$-bovine serum albumin and dansyl$_5$-ovalbumin were synthesized by reacting dansyl chloride with the appropriate protein dissolved in 0.1 M sodium carbonate buffer, pH 9.8 (Weber, 1952; Parker et al., 1967b). The degree of substitution was determined by the procedure of Mihalyi & Albert (1971) by using a molar extinction coefficient at 330 nm of 4.6×10^3 cm^{-1} M^{-1} for dansyl-protein conjugates (Parker et al., 1967a). Over a period of 7 months, five New Zealand white female rabbits were each given eight intramuscular injections of 1 mg of dansyl$_{10}$-bovine serum albumin emulsified in complete Freund's adjuvant. Serum titers were monitored by quantitative precipitation (Warner & Schumaker, 1970) with dansyl$_5$-ovalbumin. One control rabbit (no injections) and two rabbits with high titers of anti-dansyl antibody underwent plasmaphoresis as previously described (Rodwell, 1976; Schumaker et al., 1980). IgG antibody was precipitated for 2 h at room temperature from the heparinized plasma by adding a solution of saturated ammonium sulfate (SAS) to a final concentration of 40% of saturation. The precipitate was collected by centrifugation at 3000g for 10 min at 4 °C and washed twice with 40% SAS and resuspended in a volume of PBS (0.01 M potassium phosphate–0.15 M NaCl, pH 7.4) equal to one-half of the original plasma volume. The sample was dialyzed at 4 °C against PBS for several days until a clear gellike clot formed. Sometimes it was necessary to dialyze the sample at room temperature for about 2 h to induce clot formation. The clot was removed by centrifugation at 17000g for 20 min. IgG was precipitated at room temperature for 2 h by adding SAS to 35% of saturation. The precipitate was washed twice with 35% SAS, dissolved in PBS to 20 mg/mL, and dialyzed exhaustively at 4 °C. The sample was then dialyzed against 0.1 M Tris–0.5 M NaCl, pH 8, and fractionated at 4 °C on a 100 × 2.6 cm column of Sephacryl S-200 (Pharmacia, Piscataway, NJ). Typically, 8 mL of a 20 mg/mL sample was applied to the column, and 6-mL fractions were collected at a flow rate of 10 mL/h. About 50% of the applied sample was eluted in the three peak fractions (Figure 2); these fractions were pooled and dialyzed against PBS. IgG concentrations were determined spectrophotometrically by using an extinction coefficient of $E_{280} = 1.5$ cm^{-1} mL mg^{-1} (Parker et al., 1967b; Steiner & Lowey, 1966; Little & Eisen, 1968).

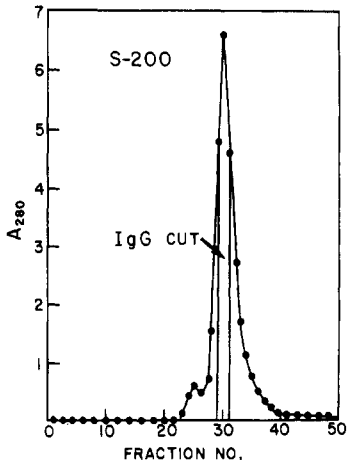

FIGURE 2: Elution profile of IgG fractionated on a 100 × 2.6 cm column of Sephacryl S-200. Fractions were quantitated by the absorbance at 280 nm; the enclosed area indicates the three peak fractions pooled for experimental measurements. Fractionation conditions were as detailed under Experimental Procedures.

Reduction and Alkylation. Selective cleavage of the single inter-heavy-chain hinge disulfide bond of rabbit IgG was achieved by mild reduction with β-mercaptoethanol (Hong & Nisonoff, 1965; Seegan et al., 1979). A 1.7 mg/mL solution of IgG in 0.05 M potassium phosphate–0.08 M NaCl, pH 7.4, was reduced with 7.5 mM β-mercaptoethanol for 45 min at room temperature. The reduced sample was alkylated in the dark with 13 mM iodoacetamide for 45 min at room temperature and then dialyzed against PBS at 4 °C. Polyacrylamide gel electrophoresis revealed that about 80% of the hinge disulfide bonds had been cleaved; no cleavage of the heavy–light interchain disulfides was detected. Also, no significant change in the sedimentation coefficient was observed upon reduction and alkylation of IgG.

Gel Electrophoresis. Sodium dodecyl sulfate–polyacrylamide gel electrophoresis was carried out according to the procedure of Laemmli (1970) with 10% acrylamide–0.27% bis(acrylamide) 1-mm resolving gels.

Analytical Ultracentrifugation. A Beckman Model E analytical ultracentrifuge equipped with a photoelectric scanner set at 280 nm was used to determine the homogeneity and sedimentation velocity of IgG samples. The scanner was interfaced to a PDP 11/45 computer with a Beckman Model 3801 data coupler as previously described (Schumaker et al., 1980). The computer produced absorbance and derivative plots as a function of radial distance. Centrifuge runs were made in PBS at 56000 or 60000 rpm at 21–22 °C with sample concentrations of about 0.5 mg/mL. Corrected sedimentation coefficients, $s^0_{20,w}$, were calculated by the standard method (Schachman, 1959).

Fluorescence Spectra. Fluorescence excitation and emission spectra were recorded with a Spex Fluorolog digital fluorometer equipped with double Czerny-Turner monochromators (Spex Industries, Metuchen, NJ).

Fluorescence Titrations. The affinity and binding homogeneity of anti-dansyl antibodies were measured by the enhancement of bound hapten fluorescence as described by Parker (1973). Titrations were performed at 20 °C with an Aminco-Bowman spectrophotofluorometer equipped with a ratio photometer and a xenon lamp magnetic arc stabilizer. Typically, 0.3 mg/mL purified IgG was titrated in PBS with ε-dansyllysine. Samples were excited at 340 nm, and fluorescence intensity was monitored at 480 nm. Corrections were made for background fluorescence and volume changes; IgG from nonimmunized control rabbits showed no detectable

binding of hapten when compared with buffer controls. The titration data were used to generate intensity, Scatchard, and Sips plots from which antibody concentrations, average intrinsic association constants, and heterogeneity indexes were calculated (Parker, 1973; Parker et al., 1967a).

Steady-State Fluorescence Polarization. Steady-state polarization measurements were made with a Perkin-Elmer MPF-44A fluorescence spectrophotometer. Unless otherwise noted, samples at 20 °C were excited with 360-nm vertically polarized light while the vertical component, I_{VV}, and the horizontal component, I_{VH}, of polarized emission intensity were monitored at 500 nm. Corrections were made for sample background fluorescence and light scattering (Shinitzky et al., 1971) and for emission monochromator polarization effects (Chen & Bowman, 1965). The steady-state anisotropy, $\bar{A}$, a measure of the average angle through which the probes rotate during their fluorescence lifetime, τ, was calculated from eq 1–3. In eq 1–3, R is the corrected steady-state polarization

$$\bar{A} = \frac{R - 1}{R + 2} \tag{1}$$

$$R = \frac{I^c_{VV}}{I^c_{VH}} \frac{I_{HH}}{I_{HV}} \tag{2}$$

$$I^c_{VV} = I_{VV} - I'_{VV} \tag{3a}$$

$$I^c_{VH} = I_{VH} - I'_{VH} \tag{3b}$$

ratio, and I'_{VV} and I'_{VH} are the emission intensities from control solutions to which the probe ϵ-dansyllysine was not added. I_{HV} and I_{HH} are, respectively, the vertical and horizontal components of emission from horizontally polarized exciting light. The limiting anisotropy, A_0, was measured at 10 °C by dissolving the sample in 80% (w/w) spectrograde glycerol (Fisher Scientific Co., Fair Lawn, NJ). We found that A_0 values determined by this method were nearly identical with those obtained by extrapolation of Perrin plots to infinite viscosity.

Nanosecond Spectroscopy—Experimental Methods. The time dependence of fluorescence intensity and anisotropy was determined by the single-photon counting technique [for reviews, see Yguerabide (1972), Wahl (1975), and Badea & Brand (1979)] with a modified Ortec nanosecond spectrometer. The instrument was equipped with an Amperex 56 DUVP photomultiplier tube and a high-pressure hydrogen discharge lamp (EEY Scientific, La Jolla, CA) pulsed at ~25 kHz (Yguerabide, 1972). Data were stored in the multichannel analyzer and later transferred to a PDP 11/05 computer for analyses. Decay curves were displayed on a Calcomp plotter interfaced to the computer. The spectrometer was calibrated for 0.838 ns per channel, and a minimum of 140 channels were used for each analysis. Decay curves for fluorescence lifetime determinations, $R(t)$, were collected by exciting the sample with vertically polarized light and monitoring the resulting fluorescence through a polarizer rotated 55° from the vertical. For this polarizer arrangement, the fluorescence intensity is independent of rotational effects (Yguerabide, 1972). Time decays for anisotropy measurements were recorded by exciting a sample with vertically polarized light while orienting the emission polarizer in a vertical, $I_{VV}(t)$, or horizontal, $I_{VH}(t)$, direction. The emission polarizer was rotated at 10-min intervals while alternately recording $I_{VV}(t)$ or $I_{VH}(t)$. All measurements were made at 20 °C and samples were excited by light selected with a Corning 7-60 band-pass filter (360-nm peak). Emission was detected through a Corning 3-71 cutoff filter. Typically, 4×10^4 peak counts were collected for lifetime decays and 8×10^4 peak counts for $I_{VV}(t)$ and $I_{VH}(t)$ decays. Moreover, we compared curves from 4×10^4 to 1.2×10^5 peak counts and found no significant differences when the decays were analyzed in terms of two exponentials according to the method described. The total counts in $I_{VV}(t)$ and $I_{VH}(t)$ curves were scaled as described by Yguerabide et al. (1970) to correct for changes in lamp intensity and frequency and to account for differences in collection times. We attempted to accurately define the decay of anisotropy by correcting for the intrinsic fluorescence of control solutions without the dansyllysine probe. Total counts from control solutions ranged from 1% to 5% of sample count rates. Decay curves for controls were recorded and subtracted from sample decays after appropriate scaling by a procedure similar to the one used to scale $I_{VV}(t)$ and $I_{VH}(t)$. We also corrected for convolution artifacts; lamp-flash profiles, $L(t)$, were recorded by removing the emission filter and scattering light from suspensions of latex beads. The constancy of $L(t)$ was checked by recording profiles before, during, and after each experiment. To correct for the photomultiplier's spectral time shift, we inserted a variable length constant impedance line (General Radio 874-LK20L) between the time-to-amplitude converter (TAC) and the anode discriminator. This arrangement allowed the lamp profile to be shifted to the appropriate position in time before it was recorded. The shift can also be performed by the computer during data analysis. Immediately before nanosecond measurements, samples were filtered through a 0.22-μm Millipore filter and spun for 10 min in an Eppendorf microfuge. Anisotropy and lifetime measurements were made by using total IgG concentrations of $\sim 2 \times 10^{-6}$ M and ϵ-dansyl-L-lysine (Pierce Chemical Co., Rockford, IL) hapten concentrations of $(1.5\text{–}3.0) \times 10^{-7}$ M. Fresh solutions were prepared for each experiment by diluting a characterized stock sample.

Nanosecond Spectroscopy—Data Analysis. The early portion of a measured fluorescence decay, $R(t)$, is distorted by the finite duration of the exciting lamp pulse, $L(t)$. $F(t)$, the undistorted time course of emission, is related to the above curves by the convolution integral (eq 4).

$$R(t) = \int_0^t L(T)F(t - T)\, dT \tag{4}$$

To determine fluorescence lifetimes, we used the method of moments (Yguerabide, 1972; Isenberg & Dyson, 1969) to obtain $F(t)$ from measured decays of $R(t)$ and $L(t)$. If $F(t)$ is represented by the two-exponential expression in eq 5, the deconvolution procedure yields values of a_1, τ_1, a_2, and τ_2.

$$F(t) = a_1 e^{-t/\tau_1} + a_2 e^{-t/\tau_2} \tag{5}$$

$F(t)$ was then convoluted with $L(t)$ (eq 4) to calculate a new function, $C(t)$. Goodness of fit was determined by calculating χ^2 defined in eq 6a. The deviation, J, is defined in eq 6b.

$$\chi^2 = \sum [R(t) - C(t)]^2 / [C(t)] \tag{6a}$$

$$J = [R(t) - C(t)] / [C(t)]^{1/2} \tag{6b}$$

For example, the deviation of $C(t)$ and $R(t)$ is plotted in the upper trace of Figure 3. An average χ^2 is given by χ^2/N where N is the number of data points. Lifetime decays were well represented by a sum of two exponentials as evidenced by χ^2/N values that ranged from 3 to 4. In eq 6a, the summation begins before the lamp peak; thus, χ^2 includes the goodness of fit for both the rising and falling portions of the curve. The anisotropy function, $A(t)$, is defined in eq 7. $I_{VV}(t)$ and $I_{VH}(t)$

$$A(t) = \frac{I_{VV}(t) - I_{VH}(t)}{I_{VV}(t) + 2I_{VH}(t)} = \frac{D(t)}{S(t)} \tag{7}$$

are the vertical and horizontal components of fluorescence, at time t, following a fast pulse of vertically polarized light. For an instantaneous or δ pulse of light, the decay of $A(t)$ is determined entirely by rotational motions of the probe and is not influenced by the lifetime τ. This assertion is strictly true only for samples displaying a single lifetime (J. Yguerabide, unpublished results). However, in the analysis which follows, we will assume that within experimental error the decay of $A(t)$ is determined entirely by rotational motions. Because the experimental lamp flash has a finite duration, it distorts $A(t)$ by distorting the early portion of the decay of both $I_{VV}(t)$ and $I_{VH}(t)$. In principle, it is possible to deconvolute $I_{VV}(t)$ and $I_{VH}(t)$ separately before calculating $A(t)$. In practice, we found this approach was not very reproducible because of statistical limitations. We have, however, obtained a high degree of precision by first calculating difference, $D(t)$, and sum, $S(t)$, functions and then deconvoluting these functions separately as described for $R(t)$ curves. χ^2/N values for these curves were usually between 5 and 7. $A(t)$ was then calculated by dividing the deconvoluted $D(t)$ and $S(t)$ two-exponential expressions. The resulting deconvoluted anisotropy curve was fit to eq 8 by using a nondeconvoluting moments program.

$$A(t) = A_0[f_s e^{-t/\phi_s} + f_L e^{-t/\phi_L}] \quad (8)$$

In eq 8, A_0 is the limiting anisotropy, f_s and f_L are the preexponential weighting factors, and ϕ_s and ϕ_L are the short and long rotational correlation times, respectively. As expected, deconvoluted anisotropy curves generated by this technique were fit very closely by two-exponential expressions ($\chi^2/N \sim 0.1$). A recent computer simulation demonstrated that the decay of anisotropy for a wide variety of probe orientations, flexibilities, and subunit sizes can be well fitted by a one- or two-exponential decay over the experimentally accessible time region (Harvey & Cheung, 1980). We found that deconvolution of $D(t)$ and $S(t)$ curves was insensitive to our choice of end channel over a range of >40 channels, which meant the curves were well-defined and, therefore, provided unique deconvoluted $A(t)$ decays with consistently well-defined correlation times. For comparison of steady-state and nanosecond data, we calculated weighted arithmetic ($\langle\tau\rangle$), second-order (τ_e), and harmonic (τ_h) mean lifetimes from our nanosecond data in Table II according to eq 9–11 where a_1

$$\langle\tau\rangle = \sum a_i\tau_i \quad (9)$$

$$\tau_e = \frac{\sum a_i\tau_i^2}{\sum a_i\tau_i} \quad (10)$$

$$\tau_h = [\sum a_i/\tau_i]^{-1} \quad (11)$$

$+ a_2 = 1$. Arithmetic, second-order, and harmonic weighted mean rotational correlation times were calculated from the nanosecond data in Table III by using equations analogous to eq 9–11. We have also derived an expression that allowed us to directly compare steady-state anisotropy and time-dependent data. The steady-state intensity, I, is related to the time-dependent intensity, $I(t)$, by eq 12 (Yguerabide, 1972).

$$I = \int_0^\infty I(t)\,dt \quad (12)$$

Substitution of eq 12 into eq 1 and 7 yields eq 13.

$$\bar{A} = \frac{\int_0^\infty A(t)S(t)\,dt}{\int_0^\infty S(t)\,dt} \quad (13)$$

The decay of total emission, $S(t)$, is independent of rotational motions and therefore can be represented by eq 5. If we represent $A(t)$ by eq 8 and perform the integrations, we derive eq 14, which relates steady-state quantities to nanosecond parameters.

$$\frac{\bar{A}}{A_0} = \frac{1}{(a_1\tau_1 + a_2\tau_2)}\left[\frac{a_1 f_s}{1/\tau_1 + 1/\phi_s} + \frac{a_1 f_L}{1/\tau_1 + 1/\phi_L} + \frac{a_2 f_s}{1/\tau_2 + 1/\phi_s} + \frac{a_2 f_L}{1/\tau_2 + 1/\phi_L}\right] \quad (14)$$

Results

Antibody Characterization. $NaDodSO_4$–polyacrylamide gel electrophoresis of purified IgG revealed only one major band of high molecular weight on overloaded gels; therefore, we were assured that the interchain disulfide bonds were intact. Samples reduced in 5% β-mercaptoethanol had two major bands with molecular weights of about 50 000 and 25 000 that corresponded to the heavy and light chains of IgG (Ahmad-Zadeh et al., 1971).

Photoelectric scanner tracings from sedimentation velocity ultracentrifuge runs clearly showed that purified samples sedimented with a single boundary. The sharpness of the boundary indicated the absence of aggregates and low molecular weight ultraviolet-absorbing contaminants. Sedimentation coefficients, $s^0_{20,w}$, of IgG isolated from rabbit 1 (R1) and rabbit 2 (R2) were 6.56 and 6.60 S, respectively.

Fluorescence spectra of free ϵ-dansyllysine in PBS exhibited a corrected excitation peak at 330 nm and a broad uncorrected emission peak near 560 nm. Antibody-bound hapten had excitation and emission maxima at about 340 and 480 nm, respectively. Our spectra agreed closely with previously published results (Yguerabide et al., 1970; Parker et al., 1967a,b). Bound ϵ-dansyllysine showed a 140–160-fold increase in fluorescence intensity when compared with free hapten.

Fluorescence titrations were performed as described under Experimental Procedures. Scatchard plots for R1 and R2 extrapolated to two binding sites per molecule; average intrinsic association constants determined from the graphs were 1.5×10^8 M^{-1} (R1) and 1.3×10^8 M^{-1} (R2). Association constants estimated from Sips plots were nearly identical with those above, and heterogeneity indexes for both samples were 0.9. The R1 and R2 IgG preparations contained 5.1% and 10.3% specific antibody, respectively. Similar titers were obtained from quantitative precipitation tests; therefore, it appears that nearly all of the anti-dansyl antibody could be precipitated with antigen.

Steady-State Polarization. At the concentrations of IgG and hapten used for nanosecond measurements (see Experimental Procedures), the steady-state polarization ratio, R, was not affected by increasing or decreasing the hapten concentration by up to 3-fold. The excitation wavelength dependence of R was measured at 20 °C from 320 to 390 nm. Over this range, the polarization ratio for sample R1 increased in a hyperbolic manner from 1.80 (320 nm) to a plateau value of 2.03 (375–390 nm). Analogous ratios for R2 ranged from 1.72 to 2.08. The limiting steady-state polarization ratio, measured at 10 °C in 80% (w/w) glycerol, ranged from 2.12 (320 nm) to 2.65 (390 nm) for R1 and from 2.03 to 2.66 for R2. The decrease in R, with decreasing excitation wavelength, is probably due to increased absorption by the second electronic band (Becker, 1969).

The results summarized in Table I indicate that R1 depolarized light at a faster rate than R2 and that reduction of the single hinge disulfide bond of sample R2 significantly increased

Table I: Steady-State Polarization of IgG

anti-dansyl antibody	R^a	$\bar{A}^b$	$A_0{}^c$
R1 native	2.000 ± 0.003	0.250	0.337
R2 native	2.041 ± 0.004	0.258	0.338
R2 red. and alk[d]	1.981 ± 0.004	0.246	0.338

[a] Mean corrected steady-state polarization ratio and standard deviation of three experiments. [b] Steady-state anisotropy calculated from R (eq 1). [c] Limiting anisotropy determined as described under Experimental Procedures. [d] R2 IgG with hinge disulfide reduced and alkylated.

Table II: Fluorescence Lifetimes of ε-Dansyllysine Bound to Anti-Dansyl Antibody[a]

anti-dansyl antibody	expt no.	a_1	τ_1 (ns)	a_2	τ_2 (ns)	χ^2/N^b
R1 native	1	0.12	1.9	0.88	24.4	3.6
R1 native	2	0.13	2.4	0.87	24.2	4.1
R2 native	3	0.11	3.2	0.89	23.8	3.9
R2 native	4	0.10	4.6	0.90	23.9	3.5
R2 red. and alk	5	0.10	3.6	0.90	24.0	3.7

[a] Parameters derived from fitting deconvoluted fluorescence decays to eq 5. [b] Average χ^2 of two-exponential convoluted curve and raw data.

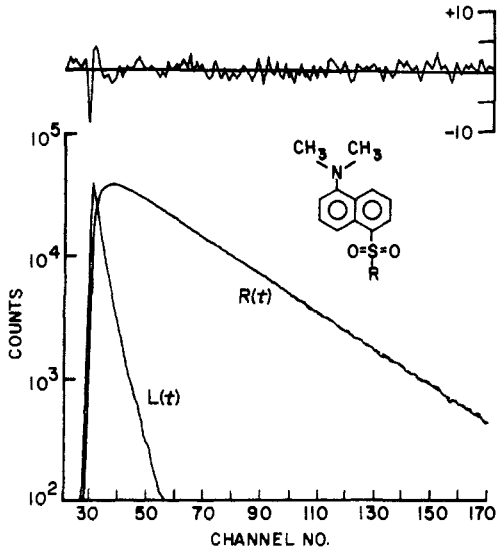

FIGURE 3: Time dependence (0.838 ns/channel) of the total fluorescence intensity, $R(t)$, of ε-dansyllysine bound in the combining sites of IgG sample R2. The two-exponential lifetime parameters (viz., experiment no. 4, Table II) were convoluted with the lamp pulse, $L(t)$, to produce the dashed curve, $C(t)$, which is superimposed on $R(t)$. Deviation of $R(t)$ (—) from the convoluted curve $C(t)$ (- - -) is shown in the upper trace.

its rate of depolarization. These differences became more dramatic when the samples were examined by nanosecond spectroscopy. Since nanosecond anisotropy decays were generated by excitation with a broad band-pass filter, the polarization wavelength dependence explains, at least in part, the lower time-dependence A_0 values (cf. Table III).

Nanosecond Spectroscopy. Deconvoluted fluorescence lifetime graphs were fit to the sum of two exponentials as outlined under Experimental Procedures. Table II shows all samples had similar decays and were dominated by a 24-ns component. As expected, almost no change in lifetime was observed upon reduction of the inter-heavy-chain disulfide bond. A typical lifetime decay and lamp profile are plotted in Figure 3. Due to the linear decays, one-exponential fits yielded τ values nearly identical with the long τ_2 obtained from

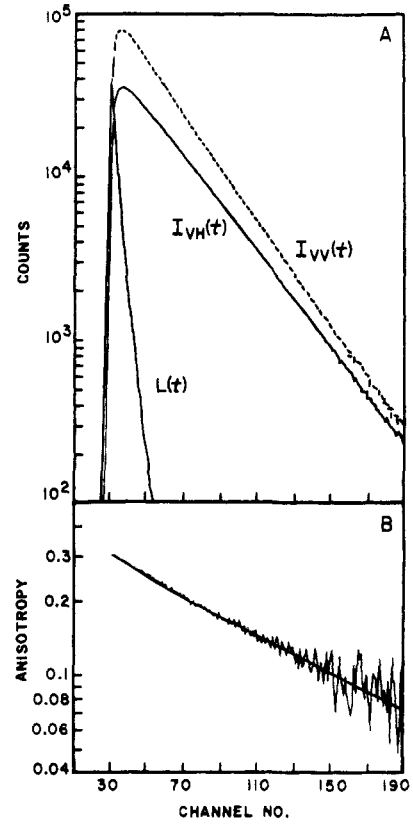

FIGURE 4: Nanosecond emission kinetics (0.838 ns/channel) of IgG R2. (A) Decay profiles of the exciting lamp pulse, $L(t)$, and scaled $I_{VV}(t)$ and $I_{VH}(t)$ decays. (B) Decay of corresponding raw and deconvoluted (smooth curve) anisotropies.

Table III: Anisotropy of IgG[a]

anti-dansyl antibody	expt no.	A_0	f_s	ϕ_s (ns)	f_L	ϕ_L (ns)	χ^2/N^b
R1 native	1	0.300	0.09	14.8	0.91	82.7	0.08
R1 native	2	0.301	0.10	13.7	0.90	83.8	0.07
R2 native	3	0.297	0.15	16.8	0.85	103.7	0.12
R2 native	4	0.302	0.12	18.0	0.88	100.3	0.12
R2 native	5	0.297	0.16	16.7	0.84	105.1	0.13
R2 red. and alk	6	0.298	0.19	14.2	0.81	90.6	0.07
R2 red. and alk	7	0.299	0.16	13.7	0.84	87.5	0.04

[a] Parameters derived from fitting deconvoluted anisotropy decays to eq 8. [b] Average χ^2 of two-exponential fit and deconvoluted anisotropy decay.

two-exponential fits. Nevertheless, the two-exponential results were preferred because they gave substantially lower χ^2 values. Since the lifetime of a dansyl fluorophore is very sensitive to its environment (Stryer, 1968), the relatively slow decay of fluorescence indicates that the ε-dansyllysine probes were bound in a hydrophobic pocket. Moreover, the lack of curvature in the decays implies that the binding pockets were providing a homogeneous environment for the probes.

The method for generating deconvoluted anisotropy curves was detailed under Experimental Procedures. Raw $I_{VV}(t)$ and $I_{VH}(t)$ profiles for R2 antibody are shown in Figure 4A, and the corresponding raw anisotropy decay curve is plotted in Figure 4B; the smooth curve (Figure 4B) is the deconvoluted anisotropy decay. Note that the beginning part of the deconvoluted curve decays slightly faster than the raw graph. Deconvolution of $A(t)$ usually decreased ϕ_s by 3–4 ns when compared with raw curves. Table III presents the results of

Table IV: Relating Steady-State and Time-Dependent Fluorescence Data[a]

anti-dansyl antibody	weighted mean τ (ns) and ϕ (ns)[b]						$\bar{A}/A_0$[c] measured	$\bar{A}/A_0$[d] calcd (eq 14)	$\bar{A}/A_0$ calcd (eq 15) with mean τ and ϕ[e]		
	$\langle\tau\rangle$	$\langle\phi\rangle$	τ_e	ϕ_e	τ_h	ϕ_h			$(\langle\tau\rangle,\langle\phi\rangle)$	(τ_e,ϕ_e)	(τ_h,ϕ_h)
R1 native	21.5	76.7	24.1	82.0	10.6	57.0	0.74	0.74	0.78	0.77	0.84
R2 native	21.8	90.8	23.4	100.7	15.5	60.1	0.76	0.76	0.81	0.81	0.79
R2 red. and alk	22.0	75.9	23.6	86.6	15.3	45.9	0.73	0.72	0.78	0.79	0.75

[a] $\bar{A}/A_0$ ratios have been rounded to two significant figures for ease of comparison. [b] Weighted mean τ and ϕ values calculated from eq 9–11 by using average nanosecond parameters derived from Tables II and III. [c] $\bar{A}/A_0$ calculated from measured steady-state data in Table I. [d] $\bar{A}/A_0$ calculated from eq 14 by using average nanosecond parameters derived from Tables II and III. [e] $\bar{A}/A_0$ calculated from eq 15 by using weighted mean τ and ϕ values from Table IV.

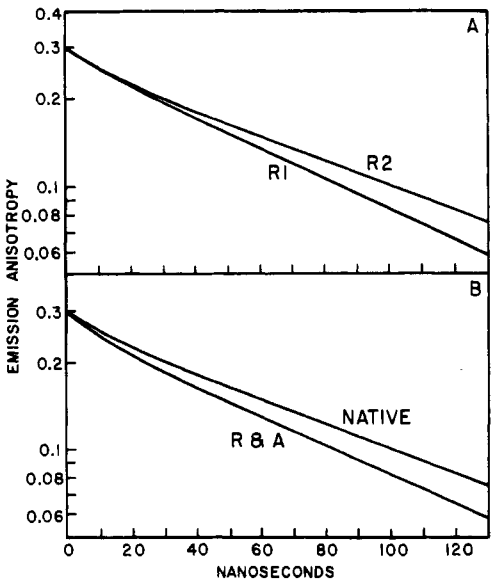

FIGURE 5: Deconvoluted emission anisotropies of IgG. (A) Decay of anisotropies of samples R1 and R2. (B) Anisotropy decay of native R2 and R2 with its hinge disulfide reduced and alkylated.

fitting deconvoluted anisotropy curves to eq 8. It is of interest that R1 had an unusually small f_s and decayed more rapidly than R2 (Figure 5A). Figure 5B shows that the cleavage of the R2's hinge disulfide resulted in a substantial increase in the rate of anisotropy decay; consequently, ϕ_s and ϕ_L both decreased, and f_s increased slightly.

Comparison of Steady-State and Nanosecond Data. Confusing results have been obtained when investigators used the steady-state technique to calculate an "average" correlation time for systems exhibiting multiple lifetimes and correlation times (Dandliker & de Saussure, 1970). The common approach has been to use the Perrin equation (eq 15) to deter-

$$\frac{1}{\bar{A}} = \frac{1}{A_0}\left(1 + \frac{\tau}{\phi}\right) \qquad (15)$$

mine an average correlation time, ϕ, from experimental steady-state values of A_0 and $\bar{A}$ and from an average lifetime, τ, obtained by either pulse or phase-shift techniques. However, this equation is strictly correct only for rigid spherical molecules with a single lifetime.

For complex systems, when ϕ is determined by the above method, the type of average represented by ϕ is not well-defined, and, therefore, the relationship between ϕ and time-dependent parameters is not clear. We have found, however, that the $\bar{A}$ and A_0 determined from steady-state measurements can be related to nanosecond data in a meaningful way if the more general expression, eq 14, is used. This equation shows that there is a complex relationship between steady-state and time-dependent polarization data. We have used average nanosecond parameters derived from the data in Tables II and III along with eq 14 to calculate the predicted steady-state $\bar{A}/A_0$ ratios. In addition, our nanosecond data were used to calculate arithmetic (eq 9), second-order (eq 10), and harmonic (eq 11) weighted mean lifetimes and correlation times. These mean τ and ϕ values were then substituted into eq 15 to calculate $\bar{A}/A_0$ ratios. Table IV clearly shows that $\bar{A}/A_0$ ratios calculated by using eq 14 agree closely with the measured steady-state ratios whereas none of the "average" methods gave satisfactory results. In fact, the $\bar{A}/A_0$ ratios calculated from second-order and harmonic mean values inverted the sample order of increasing anisotropies.

Theoretical Calculations and Discussion

Validity of New Results. Because of the significant differences between our nanosecond data and the data first obtained by Yguerabide et al. (1970), we have taken great care to assure that our new results were not influenced by artifacts.

A prolonged immunization protocol was used to produce high-affinity anti-dansyl antibody. The heterogeneity of pooled sera was avoided by using a plasmaphoresis procedure that yielded ~100 mL of plasma per bleed. Ion-exchange columns (e.g., DEAE-cellulose) were avoided during the purification procedure because we have consistently found large losses (15–35%) of IgG purified on such columns. Parker et al. (1967b) showed that ammonium sulfate fractions from rabbits injected with dansyl antigens can be fractionated on DEAE-cellulose columns into two distinct groups having different ϵ-dansyllysine binding characteristics. At the present time, we have no knowledge about possible differences in the flexibility of these subpopulations.

Our IgG preparations appeared homogeneous as judged by gel electrophoresis and sedimentation velocity profiles. The $NaDodSO_4$ gel electrophoresis patterns also indicated that the interchain disulfide bonds were intact, and the ultracentrifuge scanner tracings clearly showed that the gel filtration procedure removed all aggregates. Fluorescence titration data revealed that both R1 and R2 had average association constants of $>10^8$ M^{-1} and heterogeneity indexes of near unity. Control experiments demonstrated that there was no detectable nonspecific binding of the dansyl probe. The linearity of the semilogarithmic lifetime decay plots (e.g., see Figure 3) indicated that the probes were bound in an effectively homogeneous environment.

For our nanosecond measurements, we performed careful deconvolution, lamp-shift, and background subtraction corrections. Repeat measurements made with fresh solutions, prepared by dilution of a characterized stock sample, were reproducible (see Tables II and III). As a check for time-dependent instrumental artifacts, precise steady-state depolarization measurements were made on all our samples (Table I). Equation 14, derived under Experimental Procedures, was used to compare the steady-state and nanosecond data. As shown in Table IV, the data derived from these two inde-

pendent methods compared remarkably well.

Possible Reasons for Anisotropy Differences. The ϕ_L of 168 ns found by Yguerabide et al. (1970) is considerably longer than the ϕ_L for either of our samples, R1 or R2. Also, the f_s and ϕ_s reported by these workers are approximately twice as large as the corresponding parameters for R1 and R2. Possible reasons for these differences include the fact that Yguerabide et al. used IgG isolated by fractionation of pooled rabbit sera on DEAE-cellulose. The heterogeneity of this IgG is obvious from the curved lifetime decay [cf. the linear decay of R2 in Figure 3 with Figure 7 of Yguerabide et al. (1970)]. In addition, gel filtration was not performed for the removal of aggregates. The presence either of aggregates or of less flexible antibody populations could dramatically decrease the rate of anisotropy decay.

The decay of raw fluorescence anisotropy of our sample R2 was similar to the profile found by Chan & Cathou (1977) for anti-dansyl antibody purified of aggregates. R1 consistently exhibited a more rapid decay of anisotropy than R2. R1's decay was similar to that of reduced R2; yet electrophoresis patterns revealed that the hinge disulfide of R1 was intact. Furthermore, the sedimentation coefficients of R1 and R2 were nearly identical. Other investigators have also reported differences in depolarization rates of antibodies isolated from different rabbits (Murakami & Nakamura, 1976; Lovejoy et al., 1977).

The observed differences in the anisotropy decays for IgG antibody from different rabbits could be due to differences in hapten orientation within the binding site or to genetically determined differences in antibody structure. In their steady-state studies on IgG antibody, Murakami & Nakamura (1976) showed experimentally that, as expected from theory, the orientation of the emission transition moment with respect to the long axis of the Fab arm can produce large changes in polarization. Dudich et al. (1978) found a >50% increase in the steady-state ϕ value for pig antibodies that were unable to precipitate with antigen. If orientation effects alone are responsible for differences in the decay of fluorescence anisotropy, then the anisotropy profiles for Fab fragments from different rabbits should also be different. However, if samples differ only in their structural flexibility, the Fab fragments from the different samples should have nearly identical decays. Of course, both effects may be operating simultaneously.

Possible Modes of Depolarization. Assuming that our time-dependent data are free of artifacts, we have sought to define rotational motions of the IgG antibody molecule that could be responsible for our observed decays of fluorescence anisotropy. On the basis of the current model for IgG antibody structure that has emerged from X-ray diffraction and electron microscopy studies, we have selected likely modes of depolarization for a probe rigidly bound at the binding sites of the Fab arms. The suggested modes include the following: Fab wagging, wobbling, and twisting about the hinge region; V-module flexing at the switch peptides; and global tumbling of the entire molecule.

To determine which of these motions are compatible with the observed ϕ_s and ϕ_L, we made estimates of their rotational correlation times. It should be clear, however, that at the present time we do not have enough information to accurately predict the rotational correlation times associated with the suggested depolarizing motions. Anisotropy decays from flexible macromolecules are complex (Harvey & Cheung, 1980) and depend upon the nature of the flexible motions, segment sizes and shapes, transition dipole moment orientations, restoring forces, bend angles, and steric interactions.

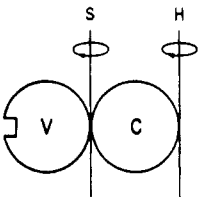

FIGURE 6: Fab antibody arm modeled by two equivalent spheres representing the V and C modules. Hypothetical switch and hinge region rotation axes are labeled S and H, respectively. Note that the switch peptides are not shown.

Because of these poorly defined complexities, we have used simple diffusion calculations merely to establish that certain likely flexible motions could occur with correlation times similar to the observed ϕ_s and ϕ_L and that ϕ_L does not seem to represent global tumbling as previously suggested.

ϕ_L Is Not Compatible with Global Tumbling. A hydrodynamically equivalent radius, r_e, of 54.2 Å was calculated for IgG by combining Stoke's law and the standard sedimentation velocity equation [Van Holde (1971), eq 4.2 and 5.3] using M = 150000, $\bar{v}$ = 0.73 mL/g, and our measured $s^0_{20,w}$ = 6.6 S. The predicted global rotational correlation time, ϕ_G, is related to the equivalent radius r_e, the solution viscosity η, the Boltzmann constant k, and the absolute temperature T by eq 16. Using this relationship, we calculated a ϕ_G of

$$\phi_G = \frac{4\pi\eta r_e^3}{3kT} \tag{16}$$

167 ns for IgG in PBS at 20 °C. A rotational time of 180 ns was obtained from electric birefringence measurements on bovine IgG at 20 °C (Riddiford & Jennings, 1967). Because of the rather compact Y-shaped structure of IgG, birefringence measurements should also provide an estimate of ϕ_G (Yguerabide et al., 1970).

These results indicate that the long correlation time for either R1 or R2 is too short to represent ϕ_G. Global tumbling should have little influence on the decay of anisotropy if the rates of intramolecular flexible motions are significantly faster than the overall tumbling and if they occur over a sufficient angular range to depolarize most of the fluorescent light. The depolarizing motions associated with ϕ_L must have a fairly large angular range because we can follow about 80% of the decay of anisotropy without observing the longer correlation time predicted for global tumbling. Lovejoy et al. (1977) were able to observe >95% of the anisotropy decay for anti-pyrene IgG and also found no decrease in slope at longer times. In other words, the different modes of Fab flexibility appear sufficient to depolarize most of the fluorescent light at a more rapid rate than global tumbling of the entire molecule.

ϕ_L Is Compatible with Fab Wagging or Wobbling. A wagging or conelike wobbling motion of the antibody arms (e.g., see Figure 1) is suggested by electron micrographs of IgG complexes (Valentine & Green, 1967; Seegan et al., 1979). These micrographs clearly show that the major site of Fab flexibility is at the hinge region. For simplicity, we first consider the antibody arm as a hydrodynamically rigid unit. Intuitively, we expect that end-over-end rotation of a free Fab fragment about a short axis through its center (switch region) would be faster than the corresponding wagging or wobbling rotation of the hinged arm in an intact IgG molecule about an axis through its hinge region. We have attempted to crudely quantitate the above argument by using the mathematical treatment of Garcia de la Torre & Bloomfield (1977, eq 19–21) to calculate the expected rotational diffusion coefficients for rotation of the model shown in Figure 6 about

the switch region axis, S, and about the hinge region axis, H. Our calculations indicate that translocation of the short rotation axis (actually there are two equivalent short axes) from the free Fab switch region to the intact IgG hinge region would decrease the rate of Fab rotation about the axis by a factor of 2.6.

The above calculation is in approximate agreement with a most recent formalism developed by Wegener et al. (1980) to calculate the rotational behavior of flexible segments hinged at their ends. If we assume that the Fab arm is a 2:1 prolate ellipsoid attached to IgG by a frictionless universal joint at a *fixed* point, then a decrease of 2.4 is calculated [see eq 30a and 34 of Wegener et al. (1980)] for the wagging and wobbling end-over-end rotational rate. In addition, Wegener et al. provide equations that include effects of translation of the joint during rotation. These equations predict that the rotational rate would decrease by a factor of 1.5 for a 2:1 ellipsoid attached by a frictionless universal joint to an identical particle [eq 40, 46, and 47a and Figure 3 of Wegener et al. (1980)]. Therefore, according to this formalism, a decrease somewhere between 1.5 and 2.4 is expected for the rotational rate of a hinged antibody arm compared to that of a free Fab fragment.

Because many of the molecular parameters required to calculate ϕ are unknown, as discussed earlier, we cannot accurately predict the rotational correlation time associated with flexible wagging or wobbling motions of the antibody arms. However, on the basis of the above discussion, we can crudely estimate ϕ. For this calculation, we ignored most of the complexities mentioned earlier and again considered the antibody arm to be attached by a frictionless universal joint. If we represent the free Fab fragment by a 2:1 prolate ellipsoid, the Perrin equations [see eq 53 and Table II of Tao (1969)] predict that the diffusion coefficient for rotations about the short (minor) axis will equal $D/1.5$ where D is the rotational diffusion coefficient for a sphere of equal volume. Using a molecular weight of 50 000, $\bar{v}$ = 0.73 mL/g, and hydration = 0.4 mL/g, we calculated $D = 7.1 \times 10^6$ s^{-1} (Yguerabide, 1972, eq 20–22). The diffusion coefficient, $D_\perp$, for rotations about the fragment's short axis is then equal to 4.7×10^6 s^{-1}. Our previous calculations predict that, for an intact IgG, the rotational diffusion coefficient for Fab end-over-end (i.e., wagging or wobbling) rotations will decrease by a factor between 1.5 and 2.4 compared to that of the free fragment; thus, for these motions, we estimate that $D_\perp$ is between 2.0×10^6 and 3.1×10^6 s^{-1}. The rotational correlation time associated with rotations about the short axis is equal to $1/(6D_\perp)$ (Tao, 1969, eq 50; Yguerabide, 1972, eq 27). On the basis of our estimates of $D_\perp$, the ϕ value corresponding to wagging or wobbling of the hinged Fab arm about the translocated short axis is therefore between 54 and 83 ns. Although greatly oversimplified, these calculations indicate that the ϕ value for such motions would be substantially longer than the single correlation times of 26–33 ns reported for free Fab fragments (Cathou, 1978; Yguerabide et al., 1970). Furthermore, since we do not expect the antibody to provide a frictionless universal joint, the anticipated "molecular friction" and structural constraints would cause an additional increase in the associated correlation time. Thus, the long rotational correlation time for either R1 or R2 appears to be compatible with wagging or wobbling motions of the Fab arms.

A recent Monte Carlo computer simulation of fluorescence depolarization by flexible macromolecules demonstrated that, except for a probe wobbling about a fixed universal joint, it is usually not possible to determine the range of bend angles from the results of a nanosecond experiment (Harvey & Cheung, 1980). Nevertheless, the fact that the flexible motions associated with ϕ_L depolarize most of the light indicates that they occur over a large angular range. Electron micrographs of antibody complexes (Valentine & Green, 1967; Seegan et al., 1979) and the ability of IgG to agglutinate large antigens suggest that the Fab arms move over a wide angle in solution. Furthermore, a recent study by Schumaker et al. (1980) revealed there is almost no strain energy associated with opening or closing of the antibody arms over a wide range of hinge angles. Therefore, it also appears that the angular range suggested for Fab wagging or wobbling is compatible with the large angular range predicted for the motions associated with ϕ_L.

The concept that wagging or wobbling motions are principally responsible for the observed ϕ_L is further supported by studies that suggest the antibody's two arms move as relatively independent units. The absence of strain energy associated with large changes in the Fab hinge angle suggests that there is little coupling between the antibody arms (Schumaker et al., 1980). X-ray diffraction studies also indicate that Fab conformations are not substantially influenced by movement of Fc regions (Edmundson et al., 1978). More recent X-ray studies showed that the hinge region connecting the antibody arms to the Fc piece has a very open structure, and no lateral noncovalent interactions between the two Fab arms were observed (Marquart et al., 1980). Of related interest are time-dependent depolarization studies on myosin that showed the correlation time associated with flexibility of the S-1 head moieties is twice as long as ϕ for tumbling of the free S-1 fragments (Mendelson et al., 1973). Furthermore, in a more recent study, Mendelson & Cheung (1978) found only a 9% increase in ϕ when one of the two myosin heads was removed. The authors concluded that "S-1 moieties act as if they pivot independently". Taken together, the above studies suggest that the antibody arms have minimal association with each other or with the Fc region and therefore should be free to move in an independent fashion. Nevertheless, the motions of the two arms probably influence each other. Wegener et al. (1980) show that for joints with incomplete flexibility "correlation coefficients arise...since an end-over-end rotation of one segment tends to displace the joint and thereby induce an end-over-end rotation of the other segment". The sign of the coefficients has an angular dependence; therefore, the motions of the Fab arms (and also the Fc region) may slightly increase or decrease the other's rotational rates, depending on the average angle between the segments.

ϕ_s Is Compatible with Fab Twisting or V-Module Flexibility. We consider twisting of an antibody arm around its long axis to be a possible fast mode of flexibility. For a free 2:1 prolate ellipsoid, rotations around the long axis are nearly twice as fast as end-over-end tumbling around the short axes (Tao, 1969). Moreover, the Fab fragment would not experience a translocation of this "twisting" axis when hinged in IgG. Thus, if the structural constraints imposed by the hinge structure are not severe, a twisting motion could produce a rapid correlation time similar to the observed ϕ_s.

Crystallographic techniques have shown that the Fab arms of IgG are composed of two globular modules connected by two switch-region peptides (Silverton et al., 1977; Marquart et al., 1980). In Figure 6, we have modeled the antibody arm (i.e., the Fab segment) by two spheres of equal radius. The V module contains the antigen binding site, and the C module contains the hinge region that connects the arm to the Fc portion of the intact molecule; switch peptides (not shown) connect the two modules.

X-ray diffraction (Huber et al., 1976; Edmundson et al., 1978), spin-label (Kaivarainen & Nezlin, 1976), and theoretical studies (McCammon & Karplus, 1977) suggest that the Fab domains exhibit restricted flexibility. The rather open switch region connecting the V and C globular modules is the proposed site of flexibility. On the basis of the V module's spherical shape and using $\bar{v}$ = 0.73 mL/g, hydration = 0.4 mL/g, and molecular weight = 25 000, we estimated a correlation time of 11.8 ns for rotation of the free module in solution [see eq 20 and 22 of Yguerabide (1972)].

Wegener et al. (1980) estimate that the rotational diffusion rate of a hinged sphere will decrease by a factor of 1.3 (identical particle) to 1.8 (fixed joint point), depending on the mobility of the particle to which the sphere is hinged. Therefore, on the basis of axis translocation alone, we roughly estimate an increase in the correlation time from 11.8 to about 15–21 ns, depending on the mobility of the C module. These values are close to the ϕ_s values observed for R1 and R2.

Our calculations indicate that the observed ϕ_s values are compatible with restricted flexing of the V module about the switch peptides or rapid twisting motions of the Fab arm around its long axis or a combination of such motions. If rapid V-module flexibility occurs, the similarity between the ϕ observed for Fab fragments (Yguerabide et al., 1970) and ϕ_s could explain the lack of curvature in the fragment's decay of anisotropy. Although we cannot calculate an exact angular range for the motions associated with ϕ_s, the small f_s values suggest that they are fairly restricted.

Discussion of the Model. Our calculations suggest that ϕ_L does not represent global tumbling of IgG and that both ϕ_s and ϕ_L are associated with flexible motions of the Fab regions. It is interesting that these motions can be separated in time by the nanosecond technique. On the other hand, the linear decay of fluorescence anisotropy observed for Fab fragments (Yguerabide et al., 1970) indicates that the rates of rotation around the long axis, end-over-end tumbling about the short axes, and possible V-module flexibility are not sufficiently different to be separated by this method for the free Fab particle.

Apparently the fast and slow flexible motions of IgG can be separated because of the increase in the correlation time associated with wagging or wobbling motions of the hinged Fab arm. This increase is most likely due to (1) a translocation of the Fab's short rotation axis from the center of the Fab fragment (switch region) to the hinge region in the IgG molecule, (2) structural constraints at the hinge, and (3) steric hindrance from the neighboring Fab and Fc globular regions. In addition, there is probably some global tumbling superimposed on the decay of anisotropy, but this effect seems to be relatively small for R1 and R2.

Interpretation of IgG nanosecond data in terms of our model would be inappropriate if strong coupling exists between Fab arm motion and global tumbling. Increased coupling, and a corresponding increase in ϕ_L, would be predicted for antibodies unable to precipitate or agglutinate antigens, or with structural alterations such as hinge deletions or aggregation. Moreover, particular transition dipole moment orientations (e.g., in certain monoclonal antibodies) could limit the amount of depolarization from flexible motions and thereby increase global coupling.

We found that the biological function of IgG and changes in flexibility upon hinge cleavage could be interpreted in terms of our model. Also, together with other studies, the depolarization changes resulting from hinge reduction provide additional support for the model.

Biological Function. Segmental flexibility seems to be an essential part of the antibody's biological function. For example, antibodies unable to precipitate with antigen were found to be less flexible than precipitating antibodies (Dudich et al., 1978). Independent movement of the antibody arms would be important for multivalent binding; after one arm is bound, the other arm must be free to rapidly locate a nearby determinant. Cross-linking of determinants also would be facilitated by the suggested modes of Fab flexibility: wagging or wobbling of the arms over a wide angular range would enable the antibody to span a variety of antigenic determinants; tight binding could then occur because V-module flexibility and Fab twisting would allow for proper alignment of the binding pockets with neighboring epitopes.

Modulation of Flexibility by Disulfide Cleavage. Cleavage of R2's hinge disulfide increased the rate of anisotropy decay (Figure 5B). Romans et al. (1977) found that disulfide reduction increased the ability of IgG to agglutinate red cells. Conversely, almost no change in sedimentation velocity (Goers et al., 1975; Seegan et al., 1979) or ultrastructure, as seen in the electron microscope (Seegan et al., 1979), occurred upon hinge reduction of monomer IgG. Also, reduction and alkylation caused no change in the conformation of IgG as judged by circular dichroism (Bjork & Tanford, 1971; Dorrington & Smith, 1972). These results imply that hinge cleavage increases the range and rate of Fab segmental flexibility without altering the antibody's global structure. Thus, the change in ϕ_L upon reduction provides additional evidence that the long correlation time does not represent global tumbling of IgG.

Parameter changes resulting from hinge cleavage can be rationalized in terms of our proposed model in which we attribute the decay of fluorescence anisotropy to segmental motions of the Fab arms. Time-dependent studies have shown that for depolarization due to a probe wobbling within a cone having a fixed base, the anisotropy decays more rapidly as the cone angle increases (Kinosita et al., 1977; Mendelson & Cheung, 1978). Although the antibody arm is not attached to a completely fixed base, a drop in ϕ_L would probably occur if, as anticipated, the Fab arm is capable of moving over a wider cone angle after hinge reduction. A decrease in steric hindrance or hinge constraints should also decrease ϕ_L. If significant, the drop in ϕ_s and corresponding increase in f_s may reflect a small increase in twisting freedom around the long Fab axis. Since hinge reduction should have little, if any, effect at the switch region, the rather small changes in ϕ_s and f_s suggest that restricted motions of the V module may also make a substantial contribution to the fast component of anisotropy.

The anisotropy changes we observed upon reduction of IgG closely parallel those found by Chan & Cathou (1977). Our weighted arithmetic mean correlation time, $\langle\phi\rangle$, decreased by 16.4% upon reduction (see Table IV), whereas we calculated a decrease of 16.1% in $\langle\phi\rangle$ from their data. Our two-exponential deconvoluted anisotropy analysis for R2 was similar to the two-exponential raw fits found by Chan and Cathou for native IgG. However, these authors reported a large *increase* in ϕ_s, f_s, and ϕ_L upon reduction of IgG. They concluded that a two-exponential analysis was the most reasonable approach to fit the data but emphasized the parameters obtained cannot be considered unique solutions. Using defined systems, Grinvald & Steinberg (1974) have shown that to choose between different sets of parameters that mathematically produce very similar curves requires additional information. On the basis of our proposed model, we find it difficult to rationalize large increases in ϕ_s and ϕ_L upon hinge reduction.

New Experiments Provide Direct Support for Our Model. If the antibody's overall rotation can be restricted without affecting its flexible motions, the resulting changes in ϕ_L will reflect the extent of global coupling. Support for our model has been obtained by examining the anisotropy decays of antibody bound by its Fc region to the C1q component of complement and to protein A (Hanson et al., 1981a,b; D. C. Hanson, J. Yguerabide, and V. N. Schumaker, unpublished experiments). These experiments provide direct evidence that ϕ_L does not represent global tumbling. A particularly striking result was found for the complex composed of four molecules of IgG and two molecules of protein A. This large complex had a ϕ_L of only 170 ns. From hydrodynamic and electron microscopic measurements, we estimated that the complex had a global rotational correlation time of $\sim$1000 ns. The new experiments also indicate that Fab flexibility is not greatly restricted by binding IgG to C1q or to protein A. This finding has biological relevance as it implies that these Fc receptors can bind antibody molecules attached to an antigen regardless of the angle between the arms.

Summary. We have proposed a more flexible model to describe the Brownian motions of IgG antibody molecules in the nanosecond time range. This model supposes that both the short and the long correlation times principally represent flexible motions of the antibody arms. A variety of evidence suggests that ϕ_s is compatible with either Fab twisting or V-module flexibility and that ϕ_L is compatible with wagging or wobbling of the Fab arms about the hinge region. The anisotropy weighting factors, f_s and f_L, suggest that the faster motions occur over small angles and that the slower wagging or wobbling motions responsible for most of the depolarization occur over a wide angular range. Depolarization changes resulting from cleavage of the hinge disulfide can be interpreted in terms of our model. Together, the suggested modes of flexibility should facilitate the formation of IgG–antigen complexes by allowing the antibody to rapidly adjust both the spacing and the orientation of its binding sites.

References

Ahmad-Zadeh, C., Piguet, J. D., & Colli, L. (1971) *Immunology 21*, 1065–1071.

Badea, M. G., & Brand, L. (1979) *Methods Enzymol. 61*, 378–425.

Becker, R. S. (1969) *Theory and Interpretation of Fluorescence and Phosphorescence*, pp 82–84, Wiley, New York.

Bjork, I., & Tanford, C. (1971) *Biochemistry 10*, 1289–1295.

Brochon, J., Wahl, P., & Auchet, J. C. (1972) *Eur. J. Biochem. 25*, 20–32.

Cathou, R. E. (1978) *Compr. Immunol. 5*, 37–83.

Chan, L. M., & Cathou, R. E. (1977) *J. Mol. Biol. 112*, 653–656.

Chen, R. F., & Bowman, R. L. (1965) *Science (Washington, D.C.) 147*, 729–732.

Dandliker, W. B., & de Saussure, V. A. (1970) *Immunochemistry 7*, 799–828.

Dorrington, K. J., & Smith, B. R. (1972) *Biochim. Biophys. Acta 263*, 70–81.

Dudich, E. I., Nezlin, R. S., & Franek, F. (1978) *FEBS Lett. 89*, 89–92.

Edmundson, A. B., Ely, K. R., & Abola, E. E. (1978) *Contemp. Top. Mol. Immunol. 7*, 95–118.

Feinstein, A., & Rowe, A. J. (1965) *Nature (London) 205*, 147–149.

Garcia de la Torre, J., & Bloomfield, V. A. (1977) *Biopolymers 16*, 1765–1778.

Goers, J. W., Schumaker, V. N., Glovsky, M. M., Rebek, J., & Muller-Eberhard, H. J. (1975) *J. Biol. Chem. 250*, 4918–4925.

Grinvald, A., & Steinberg, I. Z. (1974) *Anal. Biochem. 59*, 583–598.

Hanson, D. C., Yguerabide, J., & Schumaker, V. N. (1981a) *Hoppe-Seyler's Z. Physiol. Chem. 362*, 22.

Hanson, D. C., Yguerabide, J., & Schumaker, V. N. (1981b) *Fed. Proc., Abstr., Fed. Am. Soc. Exp. Biol. 40*, 1736.

Harvey, S. C., & Cheung, H. C. (1980) *Biopolymers 19*, 913–930.

Hong, R., & Nisonoff, A. (1965) *J. Biol. Chem. 240*, 3883–3891.

Huber, R., Deisenhofer, J., Colman, P. M., Matsushima, M., & Palm, W. (1976) *Nature (London) 264*, 415–420.

Isenberg, I., & Dyson, R. D. (1969) *Biophys. J. 9*, 1337–1350.

Kaivarainen, A. I., & Nezlin, R. S. (1976) *Biochem. Biophys. Res. Commun. 68*, 270–276.

Kinosita, K., Kawato, S., & Ikegami, A. (1977) *Biophys. J. 20*, 289–305.

Laemmli, U. K. (1970) *Nature (London) 227*, 680–685.

Little, R. J., & Eisen, H. N. (1968) *Biochemistry 7*, 711–720.

Lovejoy, C., Holowka, D. A., & Cathou, R. E. (1977) *Biochemistry 16*, 3668–3672.

Marquart, M., Deisenhofer, J., & Huber, R. (1980) *J. Mol. Biol. 141*, 369–391.

McCammon, J. A., & Karplus, M. (1977) *Nature (London) 268*, 765–766.

Mendelson, R., & Cheung, P. H-C. (1978) *Biochemistry 17*, 2139–2148.

Mendelson, R. A., Morales, M. F., & Botts, J. (1973) *Biochemistry 12*, 2250–2255.

Metzger, H. (1974) *Adv. Immunol. 18*, 169–207.

Metzger, H. (1978) *Contemp. Top. Mol. Immunol. 7*, 119–152.

Mihalyi, E., & Albert, A. (1971) *Biochemistry 10*, 237–242.

Murakami, K., & Nakamura, H. (1976) *Jpn. J. Exp. Med. 46*, 59–70.

Noelken, M. E., Nelson, C. A., Buckley, C. E., & Tanford, C. (1965) *J. Biol. Chem. 240*, 218–224.

Parker, C. W. (1973) in *Handbook of Experimental Immunology* (Weir, D. M., Ed.) Vol. 1, pp 14.1–14.25, Blackwell, Oxford.

Parker, C. W., Yoo, T. J., Johnson, M. C., & Godt, S. M. (1967a) *Biochemistry 6*, 3408–3416.

Parker, C. W., Godt, S. M., & Johnson, M. C. (1967b) *Biochemistry 6*, 3417–3427.

Riddiford, C. L., & Jennings, B. R. (1967) *Biopolymers 5*, 757–771.

Rodwell, J. D. (1976) Ph.D. Thesis, University of California at Los Angeles, Los Angeles, CA.

Romans, D. G., Tilley, C. A., Crookston, M. C., Falk, R. E., & Dorrington, K. J. (1977) *Proc. Natl. Acad. Sci. U.S.A. 74*, 2531–2535.

Schachman, H. K. (1959) *Ultracentrifugation in Biochemistry*, Chapter 4, Academic Press, New York.

Schumaker, V. N., Seegan, G. W., Smith, C. A., Ma, S. K., Rodwell, J. D., & Schumaker, M. F. (1980) *Mol. Immunol. 17*, 413–423.

Seegan, G. W., Smith, C. A., & Schumaker, V. N. (1979) *Proc. Natl. Acad. Sci. U.S.A. 76*, 907–911.

Shinitzky, M., Dianoux, A. C., Gitler, C., & Weber, G. (1971) *Biochemistry 10*, 2106–2113.

Silverton, E. W., Navia, M. A., & Davies, D. R. (1977) *Proc. Natl. Acad. Sci. U.S.A. 74*, 5140-5144.
Steiner, L. A., & Lowey, S. (1966) *J. Biol. Chem. 241*, 231-240.
Stryer, L. (1968) *Science (Washington, D.C.) 162*, 526-532.
Tao, T. (1969) *Biopolymers 8*, 609-632.
Valentine, R. C., & Green, N. M. (1967) *J. Mol. Biol. 27*, 615-617.
Van Holde, K. E. (1971) *Physical Biochemistry*, pp 81, 99, Prentice-Hall, Englewood Cliffs, NJ.
Wahl, P. (1975) *New Tech. Biophys. Cell Biol. 2*, 233-285.
Warner, C., & Schumaker, V. (1970) *Biochemistry 9*, 451-459.
Weber, G. (1952) *Biochem. J. 51*, 155-167.
Wegener, W. A., Dowben, R. M., & Koester, V. J. (1980) *J. Chem. Phys. 73*, 4086-4097.
Yguerabide, J. (1972) *Methods Enzymol. 26C*, 498-577.
Yguerabide, J., Epstein, H. F., & Stryer, L. (1970) *J. Mol. Biol. 51*, 573-590.

Modulation by Monovalent and Divalent Cations of the Guanosine-5′-triphosphatase Activity Dependent on Elongation Factor Tu†

Richard Ivell,‡ Gernot Sander,§ and Andrea Parmeggiani*

ABSTRACT: In this work, the role of monovalent (M^+) and divalent (M^{2+}) cations in the GTPase activity of elongation factor Tu (EF-Tu) is studied in systems of increasing complexity. The GTPase activity induced by kirromycin in the absence of aminoacyl-tRNA (aa-tRNA) and ribosomes requires M^+; it increases with increasing [M^+] and above 0.4 M M^+ becomes inversely proportional to the cationic radius, the order of effectivity thus being $Li^+ > Na^+ > K^+ > NH_4^+ > Cs^+ > Me_4N^+$. Its K_m is similar for all M^+ species at 0.2 M M^+ (0.2 μM) but increases in the order of cation effectivity at 2 M M^+ (up to 1.1 μM for Li^+). Addition of aa-tRNA and/or ribosomes to this system stimulates the GTPase activity at [M^+] < 0.8 M but has little effect at higher [M^+]. With both aa-tRNA and ribosomes, maximum stimulation occurs in the absence of added M^+, except for NH_4^+, whose optimum concentration is 250 mM. Thus, in the kirromycin system, increasing [M^+] can substitute for the effect of aa-tRNA and ribosomes, suggesting that the action of these components is of ionic type. In the absence of the antibiotic, in a more specific system containing Phe-tRNA^{Phe}, ribosome·poly(U), and elongation factor Ts (physiological system), the M^+ are generally inhibitory, the K_m of the reaction corresponding to the highest K_m values observed in the kirromycin system for the respective cations. The EF-Tu·kirromycin GTPase does not need free Mg^{2+} or nucleotide-bound Mg^{2+}; nevertheless, the large excess of EDTA required to eliminate the activity suggests that a tightly bound M^{2+} is essential for the active conformation of EF-Tu·kirromycin. However, neither Mg^{2+} nor Ca^{2+} or Mn^{2+} was found to be tightly bound to EF-Tu. Without free Mg^{2+}, there is a marked interdependence between [M^+] and pH in the optimum of the EF-Tu·kirromycin GTPase activity, indicative of an anionic region close to and intimately involved in the catalytic center for GTP hydrolysis on the factor. This anionic region appears to be masked by added Mg^{2+}. At 0.2 M M^+, ribosomes show a specific stimulation dependent on free Mg^{2+} of the EF-Tu·kirromycin GTPase activity, whereas at 2 M M^+, they appear to display an effect dependent solely on bound Mg^{2+}. In the kirromycin system, Mg^{2+} can be effectively replaced by the class 2A metals (Be^{2+} excepted) at low and high [M^+]. In the physiological GTPase activity, M^{2+} are absolutely required and are effective in the order $Mn^{2+} > Ca^{2+} = Ba^{2+} = Sr^{2+} > Mg^{2+}$. When their concentrations are increased, particularly that of Mg^{2+}, the requirement of the EF-Tu GTPase activity for codon–anticodon interaction is partially or wholly eliminated, suggesting an important role for divalent cations in the recognition process.

During the tRNA[1]-mediated translation of mRNA into polypeptide, elongation factor Tu (EF-Tu) is responsible for the specific emplacement of an aminoacylated tRNA into the A site of the ribosome. After the binding of the ternary complex EF-Tu·GTP·aa-tRNA to the ribosome and the associated hydrolysis of GTP, EF-Tu·GDP leaves the ribosome, thereby allowing the peptide bond formation [for reviews, see Lucas-Lenard & Beres (1974), Miller & Weissbach (1977) and Bermek (1978)]. To be recycled, the complex EF-Tu·GDP interacts with a second elongation factor, EF-Ts, which accelerates the rate of formation of the complex EF-Tu·GTP. This is then stabilized by the binding of a new molecule of aa-tRNA (Fasano et al., 1978).

The antibiotic kirromycin, which binds to EF-Tu in a stoichiometric ratio of 1:1 [Chinali et al., 1977; for a review, see Parmeggiani & Sander (1980)], modifies the conformation of EF-Tu·GDP, such that, even though the fast hydrolysis of GTP occurs nomally, EF-Tu·GDP remains fixed onto the

† From the Laboratoire de Biochimie, Laboratoire Associé No. 240 du CNRS, Ecole Polytechnique, F-91128 Palaiseau Cedex, France. *Received October 1, 1980; revised manuscript received June 2, 1981.* This work was supported by the Délégation Général à la Recherche Scientifique et Technique (Grant No. 78.7.1097) and by the Commissariat à l'Energie Atomique.

‡ Present address: Institut für Physiologische Chemie and Zellbiochemie, Universität Hamburg, 2000 Hamburg 20, Federal Republic of Germany.
§ Present address: Max-Planck-Institut für Mölekulare Genetik, D-1000 Berlin 33, Federal Republic of Germany.

[1] Abbreviations used: EF-Tu, elongation factor Tu; EF-Ts, elongation factor Ts; tRNA, transfer ribonucleic acid; tRNA^{Phe}, phenylalanine-accepting tRNA; Phe-tRNA^{Phe}, tRNA chared to 40–50% with phenylalanine; aa-tRNA, aminoacyl-tRNA; mRNA, messenger RNA; M^+, monovalent cations; M^{2+}, divalent cations; GTP, guanosine 5′-triphosphate; GDP, guanosine 5′-diphosphate; GTPase, guanosine-5′-triphosphatase; GTPase/enzyme, EC 3.6.1; EDTA, ethylenediaminetetraacetic acid; EGTA, ethylene glycol bis(β-aminoethyl ether)-*N,N,N′,N′*-tetraacetic acid; Tris-HCl, tris(hydroxymethyl)aminomethane hydrochloride.

0006-2960/81/0420-6852$01.25/0